2009 American Control Conference
Hyatt Regency Riverfront, St. Louis, MO, USA
June 10-12, 2009

Optimal Nonlinear Estimation for Aircraft Flight Control in Wind Shear

Yuanwei Jing, Jiahe Xu, Georgi M. Dimirovski, *Senior Member, IEEE*, Yucheng Zhou

***Abstract*—The continue-time unscented Kalman filter (UKF) is developed to estimate the state of a jet transport aircraft. The UKF is based on the nonlinear longitudinal aircraft equations of motion, and it is designed to provide estimates of horizontal and vertical atmospheric wind inputs. The optimal state and disturbance estimates are incorporated in feedback control laws based on the slow- and fast-time-scale subsystems of the aircraft nonlinear inverse dynamics. The UKF produces accurate estimates, and the resultant flight trajectories are very similar to those obtained with perfect state feedback. The UKF is sensitive to uncertainty in the dynamic model, but much of the lost performance can be restored by treating the uncertainty as a random disturbance input.**

I. Introduction

SEVERE low-altitude wind variability represents an infrequent but significant hazard to aircraft taking off or landing. A microburst is a strong localized downdraft that strikes the ground, creating winds that diverge radially from the impact point. The effects of microburst wind shear on airplane dynamics have recently been understood in detail, and it has been found that effective recovery from inadvertent encounters may require counterintuitive piloting techniques.

Optimal trajectory analysis (OTA) has been used to identify the limits of aircraft performance in wind shear and to determine the control strategies required to achieve such performance [1]-[5]. Computation of these trajectories requires global knowledge of the flow field. Since this is not possible in practice, OTA results are not immediately useful for real-time aircraft control. Consequently, feedback control laws employing local wind-field knowledge have been developed for near-optimal flight control [1], [6], [7].

The goal of this research is to bridge the gap between the performance achieved using OTA and that attainable using feedback control based on local wind field knowledge. The design of a feedback control law is presented in [8] based on the aircraft nonlinear inverse dynamics (NID) [9], [10]. The NID controller demonstrated safe flight through severe microbursts encountered on the final approach. It was assumed that the aircraft states were known exactly. The estimation of the aircraft state and disturbance inputs from available sensor outputs was presented in [11], in which the extended Kalman filter (EKF) is postulated as a suitable estimator structure in concert with the NID control laws.

This paper proposes an estimator structure based on the continue-time unscented Kalman filtering, which is evaluated in concert with the NID control laws. Section II is dedicated to a statement of aircraft model and equations of motion while Section III considers its nonlinear feedback control law. The estimation of the aircraft state and disturbance components for noisy sensor outputs is then considered in Section IV. In Section V, the simulation results are organized to facilitate a comparison of the UKF/NID flight trajectory with that obtained using perfect state feedback and the EKF/NID flight trajectory, as well as to illustrate the estimation performance of the UKF. Finally, the conclusion is reported in Section VI.

II. Effect of Wind Share on Airplane Dynamics

A three degree-of-freedom model of a twin-jet transport aircraft is used for this study. The aircraft has a gross weight of 38500kg and maximum takeoff thrust of 107 kN. Its aero-dynamic coefficients are complex nonlinear functions of altitude, Mach number, incidence angles, rotation rates, control deflections, configuration changes, and ground proximity. Effects of wind shear on aircraft motion and aerodynamics are modeled using the techniques described in [12]. The relevant reference frames used to describe the aircraft's position, orientation and velocity are presented in Fig. 1. Flight is assumed to take place in a vertical plane over a flat Earth, and a coordinate system fixed to the ground is defined as the inertial reference frame. On the basis of these assumptions, the equations of motion are obtained as follows.

$$\dot{\chi} = V_a \cos\gamma_a + w_\chi \tag{1}$$

$$\dot{h} = V_a \sin\gamma_a + w_h \tag{2}$$

$$\dot{V}_a = \frac{T}{m}\cos\alpha_a - \frac{D}{m} - g\sin\gamma_a - \dot{w}_\chi \cos\gamma_a - \dot{w}_h \sin\gamma_a \tag{3}$$

$$\dot{V}_a = \frac{1}{V}\left(\frac{T}{m}\sin\alpha_a + \frac{L}{m} - g\cos\gamma_a - \dot{w}_h \cos\gamma_a + \dot{w}_\chi \sin\gamma_a\right) \tag{4}$$

$$\dot{\alpha}_a = q - \dot{\gamma}_a \tag{5}$$

$$I_{yy}\dot{q} = M \tag{6}$$

The effect of wind shear on airplane energy state can be described compactly. First define the specific energy (energy per unit weight) as the sum of air-mass relative kinetic energy and inertial potential energy. Substituting from (1)-(3) yields

This work is supported by the National Natural Science Foundation of China under Grant 60274009 and Specialized Research Fund for the Doctoral Program of Higher Education under Grant 20020145007.

Jia-he Xu is with Faculty of Information Science and Engineering, Northeastern University, 110004, Shenyang, Liaoning, P.R. of China. E-mail: ellipisis@163.com

Yuan-wei Jing is with Faculty of Information Science and Engineering, Northeastern University, 110004, Shenyang, Liaoning, P.R. of China. ywjjing@mail.neu.edu.cn

Georgi M. Dimirovski is with Faculty of Engineering, Computer Engg.Dept, Dogus University of Istanbul, TR-347222 Istanbul, Rep. of Turkey. E-mail: gdimirovski@dogus.edu.tr

$$E_s = \frac{V_a^2}{2g} + h = V_a\left(\frac{T\cos\alpha_a - D}{W} - \frac{\dot{w}_\chi}{g}\cos\gamma_a - \frac{\dot{w}_h}{g}\sin\gamma_a + \frac{w_h}{V_a}\right) \quad (7)$$

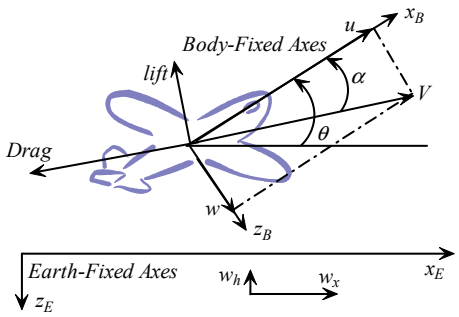

Fig. 1 Coordinate systems and reference frames for flight in wind shear.

The three wind terms, described wind shear impact on airplane energy state, may be combined into a single scalar quantity called the "*F* factor" as follow.

$$F = \frac{\dot{w}_\chi}{g}\cos\gamma_a + \frac{\dot{w}_h}{g}\sin\gamma_a - \frac{w_h}{V_a} \quad (8)$$

The effect of wind shear on airplane performance is thus expressed as an effective reduction in available specific excess power due to horizontal and vertical shears and downdrafts. Regions where *F* is negative are considered to be performance-increasing shears, while regions where *F* is positive are performance-decreasing. The aircraft's lift, drag, pitching moment and thrust are expressed as follows.

$$L = \bar{q}S_{\text{ref}}C_L \quad (9)$$

$$D = \bar{q}S_{\text{ref}}C_D \quad (10)$$

$$T = T_{\max}(V_a)\delta_T,\ 0 \le \delta_T \le 1 \quad (11)$$

$$M = \bar{q}S_{\text{ref}}\bar{c}C_M \quad (12)$$

The wind components and spatial gradients are obtained from the Oseguera-Bowles downburst model. This analytic time-invariant model represents an axisymmetric stagnation point flow, and it permits simulation of microbursts of varying size and strength through specification of the radius of the downdraft column, the maximum outflow and the altitude of maximum outflow.

III. Nonlinear Flight Control

This description of nonlinear control methods is necessarily brief. More complete treatments can be found in [13], [14]. Given a system of the form

$$\dot{x} = f(x) + G(x)u \quad (13)$$

where x is $n\times 1$ and u is $m\times 1$, we define an m-dimensional output vector

$$y = H(x) \quad (14)$$

It is possible to construct a nonlinear feedback control law that provides output decoupling of the elements of y or their derivatives such that $y^{(d)} = v$. The new control input v can be chosen to place the system poles in desired locations. The vector $y^{(d)}$ is expressed as

$$y^{(d)} = f^*(x) + G^*(x)u = v \quad (15)$$

and d is the relative degree of differentiation required to identify a direct control effect on each element of the output vector. The inverse control law then is

$$u = [G^*(x)]^{-1}[v - f^*(x)] \quad (16)$$

and the closed-loop dynamics of the system take the form

$$\dot{x} = f(x) + G(x)[G^*(x)]^{-1}[v - f^*(x)] \quad (17)$$

While the expression of the inverse control law appears simple, its implementation can be quite complex. Evaluation of the functions $f^*(x)$ and $G^*(x)$ requires that a full, d-differentiable model of the aircraft dynamics be included in the control system.

The controller can be simplified if the system can be partitioned into slow- and fast-time-scale subsystems [15]. The partition is a natural consequence of the underlying physics. For the aircraft problem, it is assumed that the pitch rate evolves q faster than the flight path γ_a and velocity V_a.

Therefore, we can partition the system (13) into slow- and fast-time-scale subsystems as follows.

$$\varepsilon\dot{x}_f = F_f(x_f, x_s) + G_f(x_f, x_s)u \quad (18)$$

$$\dot{x}_s = F_s(x_f, x_s) + G_s(x_f, x_s)u \quad (19)$$

where, $x_f = [\alpha_a\ \ q\ \ T]^T$, $x_s = [x\ \ h\ \ V_a\ \ \gamma_a]^T$; the elements of $F_f(x)$ and $F_s(x)$ are constructed using (1)-(6); ε is a positive number for the fast-time-scale subsystem.

In the slow time scale t, multiplying (18) by ε and considering the limit $\varepsilon\to 0$, since the matrix $F_f(x_f, x_s)$ has full column rank, the quasi steady state constraints $F_f(x_f, x_s) + G_f(x_f, x_s)u = 0$ are obtained. Defining

$$\varphi = \lim_{\varepsilon\to 0}\frac{F_f(x_f, x_s) + G_f(x_f, x_s)u}{\varepsilon}$$

The slow dynamics of the network take the form as follow.

$$0 = F_f(x_f, x_s) + G_f(x_f, x_s)u \quad (20)$$

$$\dot{x}_s = F_s(x_s) + G_s(x_s)u \quad (21)$$

Equation (21) is order-reduced model and the slow-time-scale subsystems of the system (13).

In the fast time scale ($\tau = t/\varepsilon$), in the limit $\varepsilon\to 0$, the dynamics of (18) take the form

$$\frac{dx}{d\tau} = F_f(x_f, x_s) + G_f(x_f, x_s)u \quad (22)$$

Equation (22) is called as boundary layer model and it is the fast-time-scale subsystems of the system (13).

The slow dynamics are thus modeled by a high index DAE, since the solution for the algebraic variables φ cannot be obtained directly from the algebraic equations.

By means of applying the dynamic inversion method to the slow- and fast-time-scale subsystems respectively, the related control quantity can be obtained. And in the slow- and fast-time-scale subsystems, the evaluation of the functions $f^*(x)$ and $G^*(x)$ requires a 4-differentiable model instead of a 7-differentiable model. Therefore, the computation progress is simpler obviously.

The controller demonstrates good recovery performance in a variety of microburst encounters when perfect state feedback is used as the basis of the control. Such state feedback would not be available in practice, it would be necessary to estimate the aircraft state and disturbance components for noisy sensor outputs. The unscented Kalman filter has been developed to accomplish this task.

IV. Optimal State Estimation

Although the extended Kalman filtering (EKF) is the most widely used filtering strategy within communication and aerospace applications, it has two well known drawbacks: (1) the first-order linearization can introduce large errors in mean and covariance of the state vector, and (2) the derivation of Jacobian matrices is nontrivial in many applications.

The unscented Kalman filter (UKF) [16] was proposed in 1990s as an improvement to EKF. The UKF is widely used in practice, ranging from multi-sensor fusion [17], target tracking [16], position determination [18], to training of neural networks [19]. And the problem of the continue-time filtering based on UKF has been recently solved in [20]. The continue-time unscented Kalman filter derives optimal aircraft state and wind component estimates for use with the NID control laws. The UKF is an optimal filter in the sense that it minimizes the variance in the estimation error associated with a nonlinear system.

A. Filter Equations for the Jet Transport

The continue-time UKF estimates the state of the jet transport aircraft using available inertial and air-data measurements. A key feature of the UKF in this application is its ability to estimate the horizontal and vertical wind components w_x and w_h. Estimates of these quantities are used as the basis of feedback control using the NID control laws.

The wind-axis equations of motion (1)-(6) are used to define the plant model for the estimator equations. There is a first-order lag in power-plant dynamics.

$$\dot{T} = \frac{T_c - T}{\tau} \tag{23}$$

where T_c is the commanded thrust, T is the actual thrust and $\tau = 2s$. The aircraft state vector is defined nominally as

$$x_a = [\chi \;\; h \;\; V_a \;\; \gamma_a \;\; \alpha_a \;\; q \;\; T]^T \tag{24}$$

The control input to the system is

$$u = [T_c \;\; \delta_E]^T \tag{25}$$

The NID control laws also require feedback of w_χ, w_h, $\dot{w}_\chi$, $\dot{w}_h$ $\ddot{w}_\chi$ and $\ddot{w}_h$. It is necessary to make these six variables part of the system state vector. The wind state vector is defined as

$$x_d = [w_\chi \;\; w_h \;\; \dot{w}_\chi \;\; \dot{w}_h \;\; \ddot{w}_\chi \;\; \ddot{w}_h]^T \tag{26}$$

In order to construct the system model, it is necessary to define the dynamics associated with the wind inputs. The equation to represent the wind components and their time derivatives is

$$\dot{x}_d = F_d x_d + w \tag{27}$$

where

$$F_d = \begin{bmatrix} 0 & 0 & 1 & 0 & 0 & 0 \\ 0 & 0 & 0 & 1 & 0 & 0 \\ 0 & 0 & 0 & 0 & 1 & 0 \\ 0 & 0 & 0 & 0 & 0 & 1 \\ 0 & 0 & 0 & 0 & 0 & 0 \\ 0 & 0 & 0 & 0 & 0 & 0 \end{bmatrix}, \quad w = \begin{bmatrix} 0 \\ 0 \\ 0 \\ 0 \\ w_1 \\ w_2 \end{bmatrix} \tag{28}$$

and w is a white, zero-mean Gaussian random variable.

$$E[w(t)] = 0, \;\; E[w(t)w^T(t)] = Q_c(t) \tag{29}$$

where $E[\bullet]$ denotes the expected value of the function.

The aircraft dynamics may thus be expressed as

$$\dot{x}_a = f(x_a, u, x_d) \tag{30}$$

where the elements of $f(\bullet)$ are constructed using (1)-(6). The complete state vector for the estimator model is defined as

$$x \triangleq [x_a \;\; x_d]^T \tag{31}$$

The combined dynamics are then written as

$$\begin{aligned} \dot{x}(t) &= f(x(t), u(t), t) + w(t) \\ &= \begin{bmatrix} \dot{x}_a(t) \\ \dot{x}_d(t) \end{bmatrix} = \begin{bmatrix} f(x_a(t), u(t), x_d(t)) \\ F_d(t) x_d(t) \end{bmatrix} + \begin{bmatrix} 0 \\ w(t) \end{bmatrix} \end{aligned} \tag{32}$$

Equation (32) describes the assumed system model used to the UKF. The disturbance input to this system is the vector w. Thus, $\ddot{w}_x$ and $\ddot{w}_h$ are modeled as zero-mean Gaussian random variables. There is a question of how to choose the elements of the matrix Q_c in (29). It has been necessary to rely on trial-and-error methods to identify suitable elements of Q_c. In effect, its components become design parameters that are adjusted to tune the filter response. The numerical values used are presented along with the simulation results.

Considered here is the form of the measurements.

$$z(t) = h(x(t), t) + n(t) \tag{33}$$

The measurement noise $n(t)$ also is assumed to be a white, zero-mean Gaussian random process that is uncorrelated with the disturbance input.

$$E[n(t)] = 0, \;\; E[n(t)n^T(t)] = R(t) \tag{34}$$

$$E[w(t)n^T(t)] = 0, \text{ for all } t \tag{35}$$

The measurement vector z is defined as

$$z = [h \;\; V_g \;\; V_a \;\; \alpha_a \;\; \theta \;\; q \;\; \dot{h} \;\; \ddot{\chi} \;\; \ddot{h}]^T \tag{36}$$

The measurement noise covariance matrix is defined as

$$R = \text{diag}(5^2, 3.6^2, 1.7^2, 0.5^2, 0.05^2, 0.05^2, 0.5^2, 0.322^2, 0.322^2) \tag{37}$$

These values are representative of state of the art inertial and air-data systems.

B. Optimal Estimator

The continue-time UKF computes minimum-variance estimates for nonlinear systems described in (32), where the vector $f(x(t),u(t),t)$ is a nonlinear function of the state x, the deterministic control input u and time. The disturbance input w is a white, zero-mean Gaussian random process with mean and covariance in (29). The disturbance is thus characterized by its spectral density matrix $Q_c(t)$. The measurement equation is also described in (33).

The expected values of the initial state and its covariance are assumed known.

$$E[x(0)] = \hat{x}_0, \;\; E[(x_0 - \hat{x}_0)(x_0 - \hat{x}_0)^T] = P_0 \tag{38}$$

According to the procedure of the UKF, the n-dimensional random variable $x(t)$ with mean $\hat{x}(t)$ and covariance $P(t)$ is approximated by the matrix of sigma points $X(t)$ selected using the following equations firstly.

$$\begin{aligned} X^{(0)}(t) &= \hat{x}(t) \\ X^{(i)}(t) &= \hat{x}(t) + \sqrt{cP}, \;\; i = 1, \ldots, L \\ X^{(i)}(t) &= \hat{x}(t) - \sqrt{cP}, \;\; i = L+1, \ldots, 2L \end{aligned}$$

where $c = \alpha^2(n + l)$ is a tuning parameter. The opposite weight ω_m is as follow.

$$\omega_m = [W_m^{(0)} \;\; \cdots \;\; W_m^{(2n)}]^{\mathrm{T}}$$

where

$$W_m^{(0)} = \frac{\lambda}{(n+\lambda)}, \;\; W_m^{(i)} = \frac{1}{2(n+\lambda)} \; (i = 1, \cdots, 2n).$$

We define the matrix W as follow

$$W = (I - [\omega_m \cdots \omega_m]) \times diag(W_c^{(0)} \cdots W_c^{(2n)}) \times (I - [\omega_m \cdots \omega_m])^{\mathrm{T}}$$

where

$$W_c^{(0)} = \frac{\lambda}{(n+\lambda)+(1-\alpha^2+\beta)}, \quad W_c^{(i)} = \frac{1}{2(n+\lambda)} \; (i = 1, \cdots, 2n).$$

The parameter λ is a scaling parameter defined as $\lambda = \alpha^2(n+l) - n$. The positive constants α, β and l are used as parameters of the method.

In the previous formulation, $z(t)$ plays the role of measured output so that the corresponding Kalman filter equations can be defined as follows.

$$\frac{dx(t)}{dt} = f(X(t),t)\omega_m + B(t)u(t) + K(t)\varepsilon(t) \tag{39}$$

$$K(t) = [X(t)Wh^{\mathrm{T}}(X(t),t) + S(t)]Q_\varepsilon^{-1}(t) \tag{40}$$

$$\frac{dP(t)}{dt} = X(t)Wf^{\mathrm{T}}(X(t),t) + f(X(t),t)WX^{\mathrm{T}}(t) + Q(t) - K(t)Q_\varepsilon^{-1}(t)K^{\mathrm{T}}(t) \tag{41}$$

where, $\varepsilon(t)$ and $Q_\varepsilon(t)$ denote the innovation of $z(t)$ and its covariance matrix, given by

$$\varepsilon(t) = [z(t) - h(X(t),t)\omega_m] \tag{42}$$

$$Q_\varepsilon^{-1}(t) = h(X(t),t)Wh^{\mathrm{T}}(X(t),t) + R(t) \tag{43}$$

The UKF is now evaluated in conjunction with the NID control laws. The UKF/NID performance is compared with the perfect state feedback and the EKF/NID.

V. Simulations Results

Aircraft encounters with microburst wind shear are considered on the final approach, during which a decision is made to abort the landing and execute a climb-out. The simulation results are organized to facilitate a comparison of the UKF/NID flight trajectory with that obtained using perfect state feedback and the EKF/NID flight trajectory, as well as to illustrate the estimation performance of the UKF.

A. Simulation during a microburst encounter

The aircraft is initialized on the glide slope at a point well outside the microburst core with an initial groundspeed of 75m/s. The microburst has a core radius of 915m, a maximum horizontal wind speed of 21m/s and a maximum outflow altitude of 46m. The initial state estimate is set equal to the actual state, so that $\hat{x}(t_0) = x(t_0)$. The covariance matrix is initialized as an identity matrix of appropriate dimension.

The disturbance input spectral density matrix Q_c is set to

$$Q_c = \mathrm{diag}(0,\ 0,\ 0,\ 0,\ 0.01,\ 0.01)$$

The selected numbers of Q_c provide a good balance between attenuating measurement noise and minimizing estimator lag.

State estimation errors are shown together with the 2σ error estimate, which is computed from the covariance matrix $P(t)$. The $\pm 2\hat{\sigma}_i(t)$ curves provide the estimated 95% confidence interval on the error associated with the state estimate $\hat{x}_i(t)$.

Figure 2 presents airspeed and angle of attack versus range from microburst core in the NID-only, the EKF/NID trajectories and the UKF/NID trajectories. Figure 4 shows the horizontal and vertical wind components experienced by the aircraft in the UKF/NID trajectory. It is evident from Fig 2 that the UKF/NID trajectory is qualitatively similar to the one obtained using perfect state feedback.

The ability to estimate the wind components is illustrated in Fig 4, which present the w_χ and w_h, estimation errors, along with the 2σ error bounds. The actual and estimated F factors in the UKF/NID trajectory are shown together in Fig. 5. The peak F experienced by the aircraft is approximately 0.4, indicating that this is a very severe microburst.

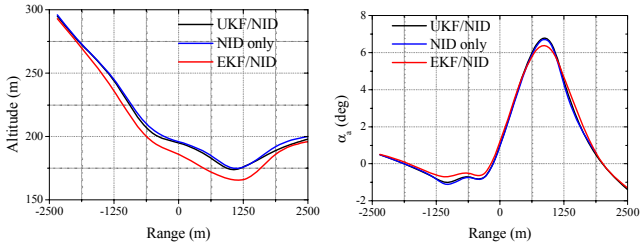

Fig.2. Altitude versus and angle of attack versus range during a microburst encounter

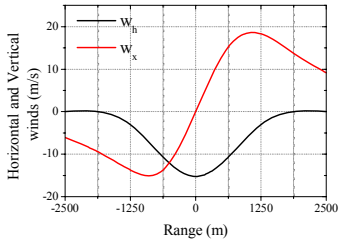

Fig.3. w_χ and w_h versus range during a microburst encounter with UKF/NID control.

It is apparent that the UKF estimates the wind components accurately. The predicted 2σ error bounds are good indicators of the accuracy of UKF, implying that the actual filter performance is consistent with the expected performance. The F-factor estimate derived from the optimal state and disturbance estimates also is quite accurate.

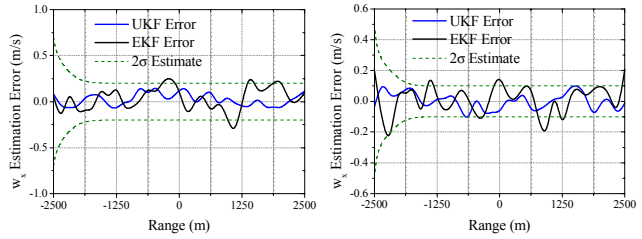

Fig.4. w_χ and w_h estimation error during a microburst encounter with UKF/NID control

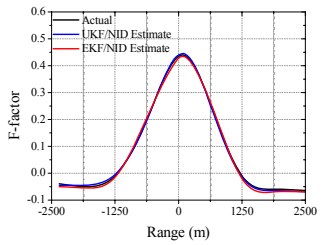

Fig.5. Actual and estimated F factor during a microburst encounter with UKF/NID control.

The results show that NID control laws can perform quite well using optimal state estimates derived from a realistic set

of measurements. However, uncertainty in the aerodynamic model poses a serious problem. The effect of uncertainty in the aerodynamic model is examined by intentionally adding an error to the lift and drag estimates used by the UKF/NID pair. The simulation is repeated using the same microburst parameters as in Figs 2-5, but now a 10% error is added to the lift and drag estimates used by both the UKF and the NID control laws. Figure 6 presents altitude and angle of attack versus range in the resultant trajectory. Wind component estimation errors in the UKF/NID trajectory are shown in Fig 7.

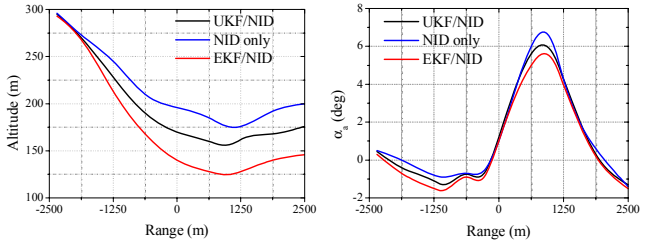

Fig.6. Altitude versus range and angle of attack versus during a micorburst encounter with UKF/NID control and 10% error in lift and drag estimates

It is apparent that the modeling errors produce a dramatic departure from the nominal flight path. The aircraft does not track the desired approach path properly in the descent portion of the trajectory. Figure 7 shows that the predicted 2σ error bounds are not good indicators for the performance of UKF. The w_χ estimation error appears to grow without bound.

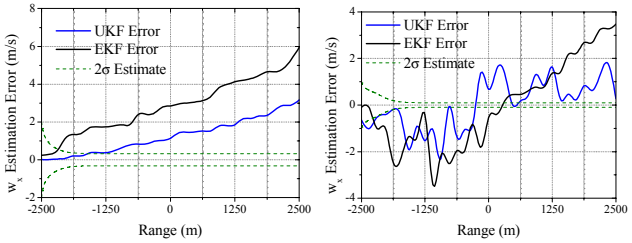

Fig.7. w_χ and w_h estimation error in the EKFINID trajectory during a microburst encounter with EKF/NID control and 10% error in lift and drag estimates.

Uncertainty in the aerodynamic model appears to be a key difficulty in the implementation of the UKF/NID estimator-controller pair. Since it is unlikely that an aircraft's aerodynamic model will ever be known exactly, it is necessary to devise a means of accommodating this uncertainty into the design. One such method is now discussed.

B. Effect of adding fictitious process noise

A simple solution for accommodating uncertainty into the design of the UKF is to add fictitious process noise $w_f(t)$ to the system model, which is treated as a Gaussian random input. The resultant model is expressed as

$$\dot{x}(t) = f(x(t),u(t),t) + w(t)$$
$$= \begin{bmatrix} \dot{x}_a(t) \\ \dot{x}_d(t) \end{bmatrix} = \begin{bmatrix} f(x_a(t),u(t),x_d(t)) \\ F_d(t)x_d(t) \end{bmatrix} + \begin{bmatrix} w_f(t) \\ w(t) \end{bmatrix} \quad (44)$$

where the fictitious input $w_f(t)$ is a Gaussian, zero-mean random variable.

$$E[w_f(t)] = 0\,,\quad E[w_f(t)w_f^T(t)] = Q_f(t) \quad (45)$$

The elements of $Q_f(t)$ are chosen to reflect the uncertainty in the time rates of change of the components of x_a that depend on L or D. For the simulation results that follow, $Q_f(t)$ is set to

$$Q_f = \text{diag}(0,\ 0,\ 0.2,\ 0.05,\ 0.05,\ 0.2,\ 0.05,\ 0.05,\ 0,\ 0) \quad (46)$$

The UKF/NID trajectory is now recomputed using fictitious process noise in the UKF plant model. As in the previous simulation, 10% errors are added to the lift and drag estimates used by the UKF/NID pair. Figure 8 shows the resultant altitude and angle of attack response respectively. Once again, the profiles obtained using the NID control law with perfect state feedback and the EKF/NID, as well as an exact model are shown for comparison purposes. Horizontal and vertical wind estimation errors in the UKF/NID flight path are shown in Fig 9. Figure 8 shows that the UKF/NID altitude and angle of attack profiles with fictitious process noise are much more similar to the NID baseline than those in Fig 6. Figure 9 demonstrate that adding the fictitious process noise restores the performance of UKF. The predicted 2σ error bounds are once again good indicators of the accuracy of the wind component estimates. The steady-state error bounds are larger in Fig 9 than in Fig 7. This may be expected, since the UKF plant model now contains uncertainty in the model itself as well as in the measurements.

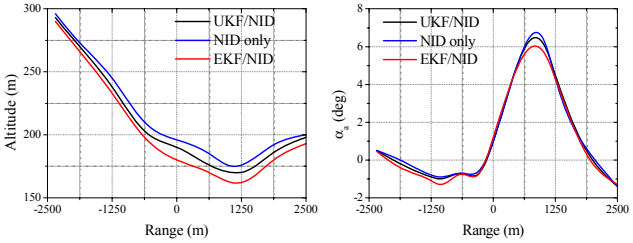

Fig.8. Altitude versus range and angle of attack versus during a microburst encounter with UKF/NID control that incorporates fictitious process noise to account for 10% error in lift and drag estimates.

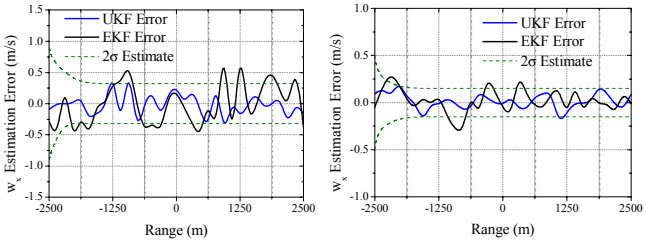

Fig.9. w_χ and w_h estimation error during a microburst encounter with UKF/NID control that incorporates fictitious process noise to account for 10% error in lift and drag estimates.

The simulation results indicate that it is possible to effectively compensate for plant model uncertainty by adding fictitious process noise to the UKF equations. The resultant flight path is similar to the one obtained using perfect state feedback with an exact aerodynamic model. The UKF/NID pair functions effectively using a realistic set of measurements and an uncertain aerodynamic model.

VI. CONCLUSION

The continue-time Unscented Kalman Filter is developed to estimate the state vector and wind disturbance inputs of a jet transport aircraft. The UKF was evaluated in concert with nonlinear control laws developed previously. Simulated flight trajectories produced using the UKF/NID pair is almost identical to those obtained using the NID control laws with perfect state feedback. The UKF produced accurate estimates of both horizontal and vertical wind inputs using a simple integral-state-model representation of the wind system. This representation makes no assumptions about the structure of the atmospheric disturbance, and it should be able to provide accurate disturbance estimates in a variety of atmospheric conditions. The introduction of fictitious process noise in the UKF equations, which treated the uncertainty as a random disturbance input, restored most of the lost performance.

Consequently, the UKF/NID control law is a good candidate for operational implementation.

REFERENCES

[1] Miele A. Optimal trajectories and guidance trajectories for aircraft flight through wind shears. *Proceedings of the 29th IEEE Conference on Decision and Control*, *Honolulu*: *HI*, 1990(2): 737-746.

[2] Mulgund S S, Stengel R F. Target pitch angle for the microburst escape maneuver. *Journal of Aircraft*, 1993(30): 826-825.

[3] Mulgund S S, Stengel R F. Optimal recovery from microburst wind shear. *Journal of Guidance, Control, Dynamic*, 1993(16): 1010-1017.

[4] Psiaki M L, Stengel R F. Optimal aircraft performance during microburst encounter. *Journal of Guidance, Control, Dynamic*, 1991(14): 440-446.

[5] Zhao Y, Bryson A E. Optimal paths through downbursts. *Journal of Guidance, Control, Dynamic*, 1990(13): 813-818.

[6] Zhao Y, Bryson A E. Control of an aircraft in downbursts. *Journal of Guidance, Control, Dynamic*, 1990(13): 819-823.

[7] Miele1 A, Wang T, Melvin W W. Guidance strategies for near optimum takeoff performance in wind shear. *Journal of Optimal Theory Application*, 1986, 50(1): 1-47.

[8] Mulgund S S, Stengel R F. Aircraft flight control in wind shear using partial dynamic inversion. *Proceedings of the American Control Conference*, *San Francisco*, 1993: 400-404.

[9] Lane S H, Stengel R F. Flight control using non-linear inverse dynamics. *Automatica*, 1988(24): 471-483.

[10] Menon P K, Chatterji G B, Cheng V H L. A two-time-scale autopilot for high performance aircraft. *Proceeding of the AIAA Guidance, Navigation and Control Conference*, *New Orleans*, 1991: 35 - 44.

[11] Sandeep S M, Robert F S. Optimal Nonlinear Estimation for Aircraft Flight Control in Wind Shear. *Automatica*, 1996, 32(1):3-13.

[12] Frost W, Bowles R. Wind shear terms in the equations of aircraft motion. *Journal of Aircraft*, 1984(21): 866-872.

[13] Isidori A. *Nonlinear Control Systems*. Springer-Verlag: Berlin, 1989.

[14] Stengel R F. Toward intelligent flight control. *IEEE Transaction on System, Man and Cybernetics*, 1993, 23(6): 1699-1717.

[15] Chow J, Kokotovic P. Two-time-scale feedback design of a class of nonlinear systems. *IEEE Transaction on Automation Control*, 1978, AC-23(3): 438- 443.

[16] Julier S J, Uhlmann J K, Durrant-Whyte H F. A new approach for filtering nonlinear systems. *Proceeding of the American Control Conference*, Washington: Seattle, 1995: 1628-1632.

[17] Ristic B, Farina A, Benvenuti D, Arulampalam M S. Performance bounds and comparison of nonlinear filters for tracking a ballistic object on re-entry. *IEE proceedings of the Radar Sonar Navigation*, 2003, 150(2): 65-70.

[18] Julier S J. The scaled unscented transformation. *The Proceedings of the American Control Conference*, *Anchorage, AK*, 2002: 4555- 4559.

[19] Wan E A, R Van Der Merwe. The unscented Kalman filter for nonlinear estimation. *Adaptive Systems for Signal Processing, Communications, and Control Symposium*, 2000: 153-158.

[20] Simo Särkkä, "On unscented Kalman filtering for state estimation of continuous-time nonlinear systems," *IEEE Trans on Automatic Control*, vol.52, no.9, pp.1631-1641, Sep. 2007.